journal

J. Am. Ceram. Soc., 77 [2] 540–46 (1994)

Equilibrium-State Density Profiles of Centrifuged Cakes

Wei-Heng Shih,*,† Wan Y. Shih,†,‡ Seong-Il Kim,§ and Ilhan A. Aksay*,‡

Department of Materials Engineering, Drexel University, Philadelphia, Pennsylvania 19104

Department of Chemical Engineering and Princeton Materials Institute, Princeton University, Princeton, New Jersey 08544-5211

Ferro Corporation, Santa Barbara, California 93117-3092

We have examined the equilibrium-state density profiles of centrifuged cakes both theoretically and experimentally. The theoretical density profiles were obtained by implementing the experimental pressure–density relationship into the general differential equation for centrifugation with appropriate boundary conditions. With a power-law pressure–density relationship, $P = \beta\phi^n$, we show that $\frac{\phi(z)}{\phi_{max}} = \left(1 - \frac{z}{z_m}\right)^{1/(n-1)}$ where ϕ_{max} is the density at the bottom of the cake, z the distance measured from the bottom of the cake, and z_m the distance at which the cake density vanishes. Experimentally, the density profiles were examined with γ-ray densitometry. The predicted density profiles are in good agreement with the experimental ones. We also show that the form $\frac{\phi(z)}{\phi_{max}} = \left(1 - \frac{z}{z_m}\right)^{1/(n-1)}$ applies to sedimentation cakes as well, provided the pressure–density relationship of sedimentation cakes is also a power-law one.

I. Introduction

PACKING-DENSITY variations in a powder compact often result in nonuniform shrinkages and/or cracking during subsequent drying and sintering. In case of dry-pressed compacts, the effect of consolidation conditions on density variations has been sufficiently detailed by theoretical models.[1] However, although recent trends have favored the use of colloidal consolidation methods in order to attain a higher degree of uniformity in packing densities, the effect of the forming methods on density variations in colloidally consolidated compacts is still poorly understood. A variety of colloidal processing methods are now utilized in shape forming. These methods can be grouped into two categories, depending on whether the starting suspension is in a dispersed or flocculated state.[2,3] A thorough discussion on the benefits of these two methods has been provided by Lange.[4] Since, in both methods, a central issue is the minimization of packing density variations, the goal of this paper is to provide a theoretical model for the variation of packing density in flocculated suspensions when the flocculated network is subjected to a nonuniform pressure field.

In prior studies, Schilling *et al.*[5] used γ-ray densitometry to study the density variation in a sedimentation cake and showed that the sediment of a flocculated alumina suspension exhibited significant density variations within the cake, whereas the sediment of a dispersed alumina suspension showed a constant-density profile. Auzerais *et al.*[6] used medical X-ray computer tomography to study the settling of dispersed and flocculated silica suspensions and obtained similar results: The sediment of a dispersed silica suspension had a fairly uniform cake density, whereas those of flocculated silica suspensions showed significant density variations within the cake.[6] Shih *et al.*[7] examined the density variations in pressure-filtered cakes with γ-ray densitometry and showed that the density profiles of pressure-filtered cakes of flocculated alumina suspensions were uniform,[7] in contrast to their sedimentation counterparts, which showed significant density variations.[5] In order to control the density uniformity in the consolidated cakes, it is essential to know how the density variation in a cake is related to the consolidation parameters such as the pressure range, the suspension condition, the particle size, and the density range.

Previous studies on sedimentation, centrifugation, or pressure filtration focused on dynamic phenomena such as transient settling of stable and weakly flocculated suspensions in sedimentation[6] or the filtration process during centrifugal or pressure filtration.[8] The emphasis has been on the movement of the particles through a suspension[6] or the flow properties during filtration.[8] In this paper, we examine the equilibrium-state density variation of a centrifuged cake under various conditions both theoretically and experimentally. By equilibrium state we refer to the stage of the centrifugation process where the cake height no longer changes. Our goal is to provide a rigorous examination of the equilibrium-state density profiles of centrifuged cakes by relating the density variations to the experimentally obtained pressure–density relationships of the cakes. The result of the present study provides not only a practical way of estimating density variations in a cake without actual densitometry measurements but also the fundamental understanding about how local density variations occur in a centrifuged cake.

It has been shown that the pressure–density relationships exhibited by the consolidated cakes can be used to characterize the consolidation behavior of suspensions under various suspension and consolidation conditions.[7,9] For the centrifuged cake of a flocculated suspension, the mean pressure $P_{s,m}$ of the cake follows a power-law dependence on the average cake density ϕ_{ave} as[7,9] $P_{s,m} = \beta\phi_{ave}^n$ for the density range the authors have worked with, where the coefficient β and the exponent n depend on the suspension pH, the materials, the particle size, and also the initial suspension density. Generally, the exponent n in this relationship increases as the degree of flocculation decreases,[7,9] or as the density increases.[7] With the pressure–density relationships obtained in the centrifugation experiments, we develop a theory that relates the density profile of a centrifuged cake to the experimentally obtained pressure–density relationships. The approach is to implement the power-law density–pressure relationship[7,9] into the general differential equation for centrifugation with appropriate boundary conditions. We show that the equilibrium-state density profile of a centrifuged cake can be

C. F. Zukoski—contributing editor

Manuscript No. 194510. Received June 2, 1993; approved October 18, 1993.
Supported by the Air Force Office of Scientific Research under Grant No. F49620-93-1-0259.

*Member, American Ceramic Society.
†Drexel University.
‡Princeton University.
§Ferro Corporation.

described by a universal form as $\frac{\phi(z)}{\phi_{max}} = \left(1 - \frac{z}{z_m}\right)^{1/(n-1)}$ where ϕ_{max} is the density at the bottom of the cake, z the distance from the bottom of the cake, z_m the distance at which the cake density vanishes, and n the exponent which appears in the pressure–density relationship.

Experimentally, we examine the density profiles with γ-ray densitometry. The predicted density profiles are in good agreement with the experimental ones. The exponent n that appears in the power-law pressure–density relationship is the most crucial variable that dictates how the local density varies in a cake. The higher the value of n, the less the local density variation in the main portion of the cake.

We organize the rest of the paper as follows. Section II contains a brief description of the experimental procedures. Section III describes the theory and the comparison with experiments. Concluding remarks are given in Section IV.

II. Experimental Procedures

The ceramic powders used in this study were α-alumina (AKP-30) powders supplied by Sumitomo Chemical Company in Osaka, Japan and boehmite powders by Vista Chemical Company in Houston, TX. The median diameter of AKP-30 was 0.4 μm. The boehmite powders were agglomerated platelike crystallites. The dry agglomerates were irregular in shape with an average size of about 65 μm as determined by optical microscopy. These agglomerates were dispersed in acidic solutions (pH 3) and partially broken up into single crystallites (50–100 Å in diameters and 10–20 Å in thickness) and largely small agglomerates (<1 μm) with application of ultrasonic energy. Powder suspensions were prepared by electrostatic stabilization. Both α-alumina and boehmite suspensions were prepared under flocculation conditions, i.e., boehmite at pH 5.5 and 7.0 and alumina at pH 7.0, respectively.

The centrifugation experiments were done on an IEC Model CL Centrifuge by DAMON/IEC Division at Needham Heights, MA. The distance from the center of rotation to the bottom of the tube was R = 13.92 cm. The centrifugation frequency ranged from ω = 48 to ω = 241, resulting in a corresponding gravitational force ranging from 32.8 to 824.3 g at the bottom of the tube, where g denotes the acceleration of gravity.

The experimental density profiles of centrifuged cakes were obtained by γ-ray transmission measurements performed with a 3.2-mm-diameter beam of collimated photons of 661 keV from cesium 137 immediately after the samples were removed from the centrifugation unit. The average density at each elevation was calculated using the Beer–Lambert law.[5]

A schematic of the centrifugation tube is shown in Figs. 1(A) and (B). Initially, the tube is filled with a suspension of density ϕ_0 and height h_0 as shown in Fig. 1(A). The suspension, after it is centrifuged for a sufficiently long time, separates into two regions; on the top is the supernatant, and at the bottom the centrifuged cake. Eventually, the system reaches an equilibrium state in which the cake height h no longer changes and the cake has an average density $\phi_{ave} = h_0\phi_0/h$. Below, we develop a theoretical model to predict the density and the pressure profiles of these cakes.

(1) Density Profiles

Let us first consider the general differential equation for centrifugation in cylindrical coordinates:[8]

$$\frac{dP_s}{dr} + (1 - k_0)\frac{P_s}{r} = \Delta\rho\phi\omega^2 r + \frac{\eta\phi_l}{2\pi\kappa r}\left(\frac{q_l}{\phi_l} - \frac{q_s}{\phi}\right) \quad (1)$$

where r denotes the distance from the center of rotation, P_s the compressive pressure on the network in the cake, ϕ_l and $\phi = 1 - \phi_l$ the volume fraction of the fluid and that of the solid, respectively, $\Delta\rho$ the mass density difference between the solid and the fluid, ω the angular centrifugation frequency, η the viscosity of the fluid, κ the permeability of the cake, q_l the flux of the fluid, q_s the flux of the solid, and k_0 the coefficient of lateral pressure defined as the ratio of the horizontal pressure to the vertical pressure. Cakes are similar to soils. It is known in soil mechanics that the compressive pressure on the solid network is not uniform in all directions. The coefficient k_0 is an empirical way of taking into account the directional dependence of the compressive pressure acting on the particulate network. A typical value of k_0 for granular materials ranges from 0.4 to 0.7.

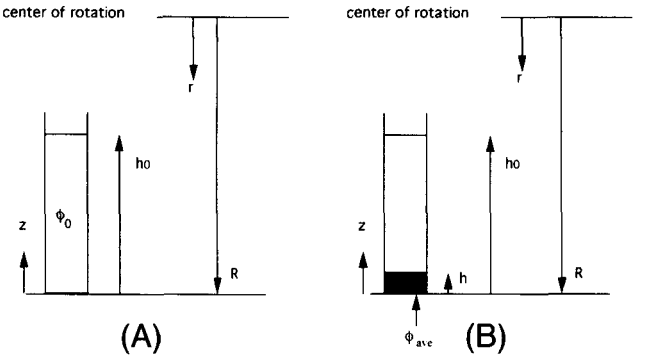

Fig. 1. Schematic of the centrifugation tube (A) with an initial suspension of density ϕ_0 and an initial suspension height h_0 and (B) at the final state, in which the suspension is separated into two regions with the supernatant on the top and the cake with an average density ϕ_{ave} and a height h that no longer changes. The density profile of a centrifuged cake in the final state is the focus of this study.

In the equilibrium state, the cake height no longer changes, indicating that there is neither material flow nor fluid flow, i.e., $q_s = q_l = 0$. Therefore, the second term on the right-hand side of Eq. (1) can be neglected and Eq. (1) becomes

$$\frac{dP_s}{dr} + (1 - k_0)\frac{P_s}{r} = \Delta\rho\phi\omega^2 r \quad (2)$$

In order to proceed further, we need to know the relationship between the compressive pressure P_s and the solid volume fraction ϕ so that a differential equation between ϕ and r can be obtained. As mentioned earlier, the mean compressive pressure $P_{s,m}$ of a flocculated centrifuged cake is a power-law function of the average density ϕ_{ave},[7,9] namely

$$P_{s,m} = \beta\phi_{ave}^n \quad (3)$$

where $P_{s,m} = \frac{1}{2}(R - \frac{h}{2})\omega^2\Delta\rho h_0\phi_0$, with R = 13.92 cm being the distance from the bottom of the cake to the center of rotation as depicted in Figs. 1(A) and (B). The values of the coefficient β and the exponent n for alumina centrifuged cakes at pH 7.0 and for boehmite cakes at pH 7.0 and 5.5 are listed in Table I. Also listed in Table I is the initial suspension density ϕ_0. The power-law pressure–density relationships of flocculated centrifuged cakes are also evident in other suspension systems such as polystyrene and clay.[10] As shown in Table I, the values for β and n not only depend on the suspension pH, and the characteristics of the particles but are also sensitive to the initial suspension density as characteristic of the nonequilibrium nature of a flocculated system.[7,9] The value for n tends to increase as the cake density increases; the boehmite cake at pH 5.5 with ϕ_0 = 2.25 vol% has a higher n than the one with ϕ_0 = 0.88 vol%. Note that the cake density ranges that Eq. (3) describes are much higher than the percolation threshold densities of these systems. Therefore, the scaling behavior of pressure with respect to density in these density ranges is not due to the percolation effect near a percolation threshold. Rather, the power-law dependence of $P_{s,m}$ on ϕ_{ave} is a manifestation of the fractal nature of the flocs that pack to form the cake[11] and is indicative

Table I. Values of β, n, ϕ_0, and h_0, for Alumina at pH 7.0 and Boehmite Centrifuged Cakes at pH 7.0 and 5.5*

	β (MPa)†	n‡	ϕ_0 (vol%)§	h_0 (cm)¶
Alumina, pH 7.0	1.73×10^2	8.9	14.82	7.88
Boehmite, pH 7.0	1.33×10^3	3.6	0.88	8.1
Boehmite, pH 7.0	1.364×10^3	4.0	2.25	7.6
Boehmite, pH 5.5	0.46	1.44	0.94	8.22

*The value of both β and n may differ as the initial suspension density changes.[13] †β is the coefficient in the pressure–density relationship. ‡n is the exponent in the pressure–density relationship. §ϕ_0 is the density of the initial suspensions. ¶h_0 is the height of the initial suspensions.

of the lack of network restructuring that occurs in pressure filtration.[7,9,12] Besides the influence from the initial suspension density, the exponent n is also closely related to the fractal dimension of the flocs that pack to form the cake. Generally, the value of n decreases as the degree of flocculation increases. Among the three suspension conditions represented here, the boehmite suspensions at pH 5.5 are the most strongly flocculated, as evidenced by their linear viscoelasticity and low gelation densities.[11] The boehmite suspensions at pH 7.0 are the second most strongly flocculated, and the alumina suspensions at pH 7.0 are the least strongly flocculated among the three. As we will show below, the density profiles of these cakes are closely related to the n value. Using Eq. (3) to approximate the relationship between P_s and ϕ, we obtain

$$\frac{dX}{dr} + \frac{n-1}{n}(1-k_0)\frac{X}{r} = \frac{n-1}{n}\frac{\Delta\rho}{\beta}\omega^2 r \tag{4}$$

where $X = \phi^{n-1}$. The solution to Eq. (4) is $X = a_1 r^2 + a_2 r^{-b}$, and the density as a function of r is then

$$\phi(r) = [a_1 r^2 + a_2 r^{-b}]^{1/(n-1)} \tag{5}$$

where $a_1 = \dfrac{(n-1)\omega^2(\Delta\rho/\beta)}{2n + (n-1)(1-k_0)}$, $b = \dfrac{n-1}{n}(1-k_0)$, and a_2 a constant to be determined by the boundary conditions. The values for a_1 and b for alumina and boehmite centrifuged cakes at various frequencies ω are listed in Table II. The quantity a_1 can be readily calculated using the input from the centrifugation experiment. The quantity b involves k_0, which ranges from 0.4 to 0.7. Even though the actual value of k_0 is uncertain, we find that the calculated density profiles are insensitive to the choice of k_0. The values for b listed in Table II are calculated with $k_0 = 0.5$.

If we let z denote the distance measured from the bottom of the cake as depicted in Figs. 1(A) and (B), the density as a function of z is then expressed as

$$\phi(z) = [a_1(R-z)^2 + a_2(R-z)^{-b}]^{1/(n-1)} \tag{6}$$

Note that $r = R - z$ is an approximation. At a given elevation z, the distance of a point on the cross section of the tube to the center of rotation r depends not only on z but also on the lateral position of that point. However, it is a good approximation as long as both the diameter of the tube and the height of the cake are much smaller than R, which is true under the experimental conditions. In a centrifugation process, the supernatant will always be present, as illustrated in Fig. 1(B). Since the solid content in the supernatant is negligible, let us assume that the supernatant has $\phi = 0$. Thus, the density of the top portion of a centrifuged cake must drop significantly to merge with that of the supernatant at some point. If we let z_m be the distance at which ϕ vanishes, the density profiles must obey the boundary conditions that

$$\phi(z_m) = 0 \tag{7}$$

and that

$$\int_0^{z_m} \phi(z)dz = \phi_0 h_0 \tag{8}$$

With the known values of a_1 and b and the boundary condition Eqs. (7) and (8), we solve for a_2 and z_m, and, thus, the entire density profile. The obtained values of a_2 and z_m for alumina centrifuged cakes at pH 7.0 and boehmite cakes at pH 5.5 and 7.0 are listed in Table II. Also listed in Table II for comparison are the visual cake heights, h. The density profiles for alumina and boehmite centrifuged cakes at different frequency settings calculated using the parameters listed in Tables I and II are shown in Figs. 2–4. Also plotted are the density profiles obtained by γ-ray densitometry at $\omega = 241$ as full circles. Within the experimental uncertainty of γ-ray densitometry measurements, the theoretical density profiles of alumina cake at pH 7.0 and those of boehmite at pH 7.0 and 5.5 with $\omega = 241$ agree well with the corresponding experimental ones. The positions of the visual cake tops, h, are also shown: open triangles represent those for $\omega = 241$, open squares for $\omega = 175$, and the open circle for $\omega = 48$. The calculated z_m may or may not coincide with the visual cake height h. For the alumina and the boehmite cakes at pH 7.0, both of which have a large n, z_m is close to h. For the boehmite cakes at pH 5.5, which have a smaller n, the difference between z_m and h becomes substantial. The reason for the large difference between z_m and h for the boehmite cake at pH 5.5 is as follows. From Fig. 4, we can see that for the boehmite cake at pH 5.5, from $z = h$ to $z = z_m$, the predicted profile shows a very low-density tail and the density range in the tail region, $h < z < z_m$, is below the sensitivity of the densitometer. It is conceivable that the tail region cannot be detected accurately. This is in agreement with the experimental observation that at pH 5.5, the boundaries between the boehmite cakes and the supernatant are diffuse and the supernatant cloudy. In contrast, the predicted profiles for the alumina cakes and the boehmite cakes at pH 7.0 do not have low-density tails. The absence of a low-density tail in the predicted profiles is again in agreement with the observation of sharp cake-supernatant boundaries for these two cases, which consequently gives rise to the close agreement of the calculated z_m with the position of the visual cake top h for these cases.

If we let ϕ_{max} be the density at the bottom of the cake, the relative density $\phi(z)/\phi_{max}$ may be expressed as a function of the relative distance z/z_m as follows. The constant a_2 is related to z_m through Eq. (7) as

$$a_2 = -a_1(R - z_m)^{2+b} \tag{9}$$

Inserting Eq. (9) into Eq. (6), we express $\phi(z)$ and ϕ_{max} as

Table II. Values of b, a_1, z_m, h, α, and γ

	ω*	b†	a_1†	a_2†	z_m (cm)†	h (cm)‡	α†	γ†
Alumina, pH 7.0	48	0.444	1.41×10^{-6}	-3.84×10^{-4}	4.0	3.87	0.207	0.98
	175	0.444	1.87×10^{-5}	-6.48×10^{-3}	2.98	2.82	0.154	0.98
	241	0.444	3.53×10^{-5}	-1.32×10^{-2}	2.66	2.66	0.138	0.98
Boehmite, pH 7.0	175	0.37	1.41×10^{-6}	-2.69×10^{-4}	4.4	4.04	0.23	1.03
	241	0.37	2.66×10^{-6}	-6.20×10^{-4}	3.7	3.35	0.196	1.03
Boehmite, pH 5.5	175	0.153	189×10^{-3}	−0.156	6.15	3.91	0.254	1.25
	241	0.153	3.58×10^{-3}	−0.553	3.53	1.55	0.146	1.25

*ω is centrifugation frequency. †As defined in text. ‡h is visual cake height.

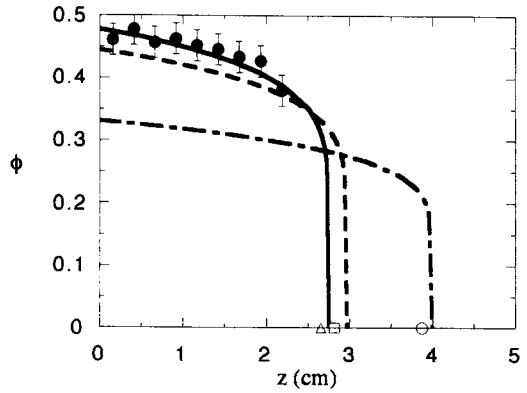

Fig. 2. Theoretical density profiles of flocculated alumina centrifuged cakes at pH 7.0. The solid line represents $\omega = 241$, the dashed line $\omega = 175$, and the broken line $\omega = 48$. Also shown are the experimental profile obtained by γ-ray densitometry at $\omega = 241$ (full circle) and the positions of the visual cake top indicated by the open triangle for $\omega = 241$, the open square for $\omega = 175$, and the open circle for $\omega = 48$. The theoretical density profile at $\omega = 241$ agrees very well with the experimental one.

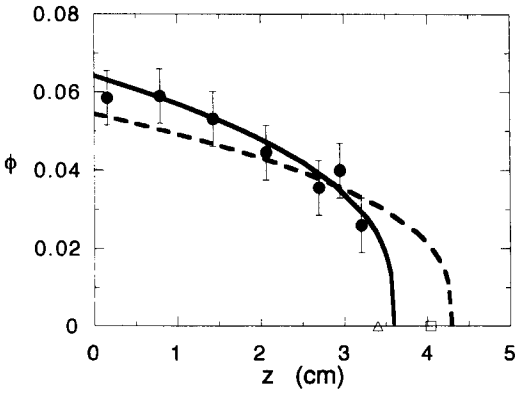

Fig. 3. Theoretical density profiles of flocculated boehmite centrifuged cakes at pH 7.0. The solid line represents $\omega = 241$, the dashed line $\omega = 175$. Also shown are the experimental profile obtained by γ-ray densitometry at $\omega = 241$ (full circles) and the positions of the visual cake top indicated by the open triangle for $\omega = 241$, the open square for $\omega = 175$. Within the experimental error bar, the theoretical density profile at $\omega = 241$ agrees very well with the experimental one.

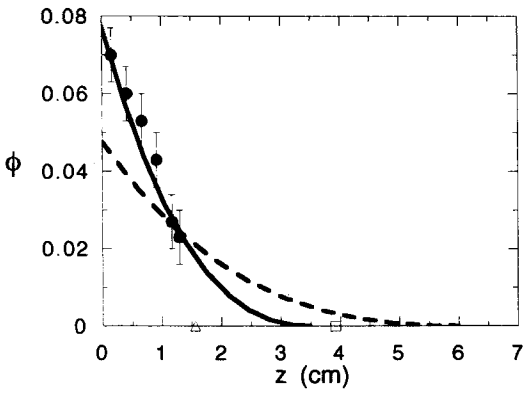

Fig. 4. Theoretical density profiles of flocculated boehmite centrifuged cakes at pH 5.5. The solid line represents $\omega = 241$, the dashed line $\omega = 175$. Also shown are the experimental profile obtained by γ-ray densitometry at $\omega = 241$ (full circles) and the positions of the visual cake top indicated by the open triangle for $\omega = 241$, the open square for $\omega = 175$. The long tail in the top portion of the cake that extends into the supernatant agrees very well with the observations of a cloudy supernatant and the diffusiveness of the cake–supernatant boundary.

$$\phi(z) = a_1[-(R - z_m)^{2+b}(R - z)^{-b} + (R - z)^2]^{1/(n-1)} \tag{10}$$

and

$$\phi_{max} \equiv \phi(z = 0) = a_1[-(R - z_m)^{2+b} R^{-b} + R^2]^{1/(n-1)} \tag{11}$$

respectively. The relative density $\frac{\phi(z)}{\phi_{max}}$ can then be related to $\frac{z}{R}$ and $\frac{z_m}{R}$ as

$$\left(\frac{\phi(z)}{\phi_{max}}\right)^{n-1} = \frac{\left(1 - \frac{z}{R}\right)^2 - \left(1 - \frac{z_m}{R}\right)^{2+b}\left(1 - \frac{z}{R}\right)^{-b}}{1 - \left(1 - \frac{z_m}{R}\right)^{2+b}} \tag{12}$$

Since both z and z_m are much smaller than R, the right-hand side of Eq. (12) can be expanded in terms of both z/R and z_m/R. To the first order in z/R and z_m/R, we arrive at a simple equation that relates the relative density $\phi(z)/\phi_{max}$ to the relative distance z/z_m as

$$\frac{\phi(z)}{\phi_{max}} \cong \left(1 - \frac{z}{z_m}\right)^{1/(n-1)} \tag{13}$$

The contribution of higher-order terms in z/R and z_m/R is negligible. For example, if we expand the right-hand side of Eq. (12) to the second order of z/R and z_m/R, we obtain

$$\left(\frac{\phi(z)}{\phi_{max}}\right)^{n-1} \cong 1 - (1 + \alpha)\frac{z}{z_m} + \alpha\gamma\left(\frac{z}{z_m}\right)^2 \tag{14}$$

where $\alpha = \frac{(b + 1)z_m}{2R}$ and $\gamma = \frac{b + 3}{(b + 1)(b + 2)}$. The values of α and γ for alumina and boehmite centrifuged cakes are also listed in Table II. Here, γ is close to unity and α is much smaller than unity, the correction due to the terms $\alpha\frac{z}{z_m} + \alpha\gamma\left(\frac{z}{z_m}\right)^2$ is negligible even near z_m. Thus, practically, Eq. (13) represents a universal description for the density profiles of centrifuged cakes, provided the compressive stress is a power-law function of the cake density. The exponent n in the pressure–density relationship is the critical parameter which dictates how the relative density $\phi(z)/\phi_{max}$ changes with the relative distance z/z_m.

To compare both the calculated density profiles and the experimental ones with Eq. (13), we first replot all the density profiles in Figs. 2–4 as $\phi(z)/\phi_{max}$ versus z/z_m as in Fig. 5. There are three sets of curves in Fig. 5. Set (a) is for alumina cakes at pH 7.0. The solid line, the open triangles, and the open squares represent the calculated curves for $\omega = 241$, 175, and 48, respectively. The full diamonds represent the experimental data points. Set (b) is for the boehmite cakes at pH 7.0. The solid line and the open diamonds represent the calculated curves for $\omega = 241$ and 175, respectively. The full circles represent the experimental data points. Set (c) is for the boehmite cakes at pH 5.5. The solid line and the open circles represent $\omega = 241$ and 175. The full squares represent the experimental points. Clearly, all the curves for alumina cakes represented in Fig. 2 collapse onto one single curve, i.e., curve (a), all the curves for boehmite cakes at pH 7.0 represented in Fig. 3 collapse onto curve (b), and all the curves for boehmite cakes at pH 5.5 represented in Fig. 4 collapse onto curve (c). Figure 5 shows that for cakes that have the same exponent n, the relative density change $\phi(z)/\phi_{max}$ has a universal dependence on z/z_m.

To compare the universal $\phi(z)/\phi_{max}$ vs z/z_m as curves shown in Fig. 5 with Eq. (13), we replot the three curves of Fig. 5

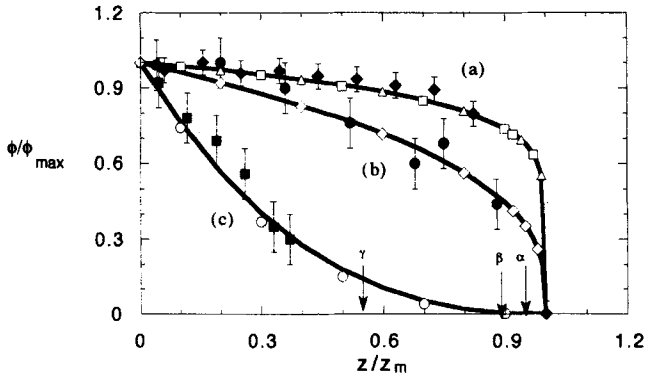

Fig. 5. $\phi(z)/\phi_{max}$ vs z/z_m. Set (a) is for alumina at pH 7.0. The solid line, the open triangles, and the open squares are calculated values for $\omega = 241$, 175, and 48, respectively. The full diamonds are the experimental values at $\omega = 241$. Set (b) is for boehmite at pH 7.0. The solid line and the open diamonds are the calculated values for $\omega = 241$ and 175, respectively, and the full circles are the experimental values at $\omega = 241$. Set (c) is for boehmite at pH 5.5. The solid line and the open circles are for the calculated values at $\omega = 241$ and 175, respectively, and the full squares are the experimental values at $\omega = 241$. The arrows indicate the positions of the experimental visual cake tops at $\omega = 241$: α for alumina at pH 7.0, β for boehmite at pH 7.0, and γ for boehmite at pH 5.5

in Fig. 6(A) as solid line (a) for alumina cakes, solid line (b) for boehmite cakes at pH 7.0, and solid line (c) for boehmite cakes at pH 5.5. Also plotted are open circles representing $\left(1 - \frac{z}{z_m}\right)^{1/(n-1)}$ at selected values of $\frac{z}{z_m}$. To better see the universality of Eq. (13), we replot Fig. 6(A) as $\left(\frac{\phi(z)}{\phi_{max}}\right)^{n-1}$ vs $\frac{z}{z_m}$ in Fig. 6(B), where the open circles represent curve (a), the open squares curve (b), and the crosses curve (c) of Fig. 6(A). For all cases, $\frac{\phi(z)}{\phi_{max}}$ is indeed well described by $\left(1 - \frac{z}{z_m}\right)^{1/(n-1)}$. Meanwhile, Fig. 6(A) shows that the relative density drop within the main portion of the cake, e.g., $0 < z < 0.8z_m$, increases as the value of n decreases. Note that $n = 2$ is a boundary for the shapes of the density profiles. For $n > 2$, such as in the alumina cakes at pH 7.0 and boehmite cakes at pH 7.0, $1/(n-1)$ is smaller than unity, and thus the $\phi(z)/\phi_{max}$ vs z/z_m curve is a convex one. For $n < 2$, such as in the boehmite cakes at pH 5.5, $1/(n-1)$ is greater than unity and therefore, the $\phi(z)/\phi_{max}$ vs z/z_m curve is a concave one. The result of a concave $\phi(z)/\phi_{max}$ vs z/z_m curve is that the cake–supernatant boundary tends to be diffuse and the supernatant cloudy as observed in the boehmite system at pH 5.5.

As for cakes that have the same n value but are centrifuged at different frequencies, the consequence of the universal dependence of $\phi(z)/\phi_{max}$ on z/z_m is that the density gradient will increase as the average cake density increases with the increasing centrifugation frequency, due to an increase in ϕ_{max} and a decrease in z_m with the increasing centrifugation frequency, both of which contribute to the increase in the density gradient. Indeed, this is clearly shown in Figs. 2–4.

(2) Pressure Profiles

Since the calculated density profiles are based on the use of Eq. (3) between the mean pressure $P_{s,m}$ and the average density ϕ_{ave} of the cakes rather than that between the actual local pressure and the actual local density, one may question whether Eq. (3) can represent the relationship between the local density and the local pressure. One way to check this is to compare the stress

$$P_s(z) = \Delta\rho\omega^2 \int_{z_m}^{z} (R - z_1)\,\phi(z_1)\,dz_1 \tag{15}$$

which is the compressive stress at position z due to the weight of the cake above z, with the stress

$$P(\phi(z)) = \beta(\phi(z))^n \tag{16}$$

which is the compressive stress at position z due to the local density $\phi(z)$ according to the pressure–density relationship Eq. (3). If Eq. (3) can indeed approximate the relationship between the local density and the local pressure, $P(z)$ must agree with $P(\phi(z))$. To see how well $P_s(z)$ compares with $P(\phi(z))$, we plot both $P_s(z)$ and $P(\phi(z))$ as a function of z for the alumina cakes at pH 7.0 with $\omega = 241$ in Fig. 7, those for the boehmite cakes at pH 7.0 with $\omega = 241$ in Fig. 8, and those for the boehmite cakes at pH 5.5 with $\omega = 241$ in Fig. 9. The solid lines represent $P_s(z)$ and the open circles $P(\phi(z))$ at selected values of z. $P(\phi(z))$ is computed according to Eq. (16) with the calculated density profiles $\phi(z)$ as the input. For all three cases, $P(\phi(z))$ agrees very well with $P_s(z)$, indicating that Eq. (3) can indeed approximate the relationship between the local pressure and the local density in the cake. One of the reasons that Eq. (3) can be used to represent the relationship between the actual pressure and the actual density is that the relative density profiles $\phi(z)/\phi_{max}$ have a universal dependence on the relative distance z/z_m as depicted by Eq. (13). Thus, as long as one defines ϕ_{ave} and $P_{s,m}$ systematically for all cakes as we have done, the relationship between

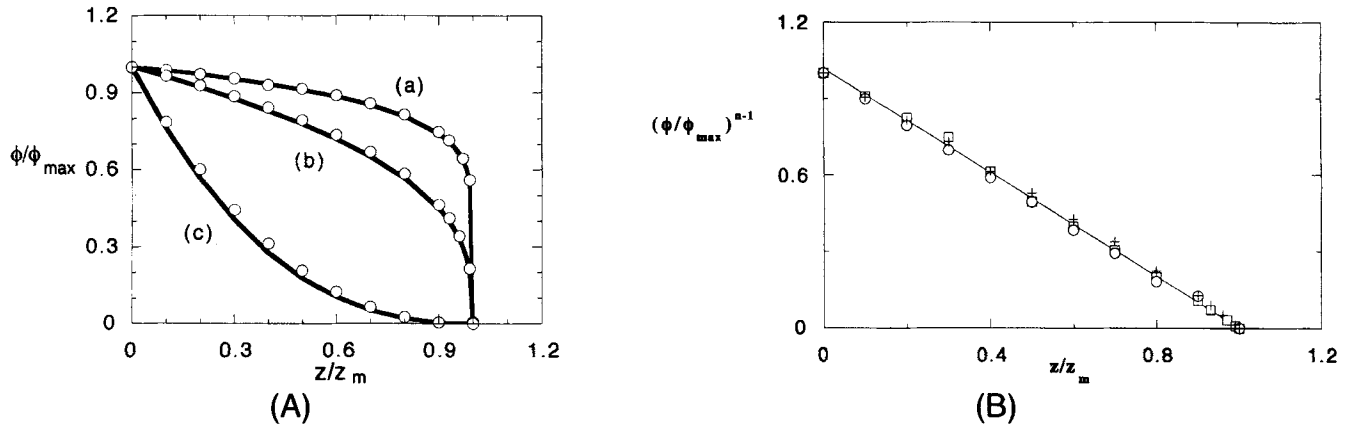

Fig. 6. (A) Comparison of $\phi(z)/\phi_{max}$ with $(1 - z/z_m)^{1/(n-1)}$. The solid lines are replotted from Fig. 5. The open circles represent $(1 - z/z_m)^{1/(n-1)}$ at selected values of z/z_m. (B) $(\phi(z)/\phi_{max})^{n-1}$ vs z/z_m. The open circles represent curve (a), the open square curve (b) and the crosses curve (c) of Fig. 6(A).

ϕ_{ave} and $P_{s,m}$ will be similar to that between the actual pressure and the actual density.

Since $P(\phi(z)) = \beta(\phi(z))^n$ can well represent the local pressure, we will then use $P(\phi(z))$ as $P(z)$ for the discussion below. Substituting Eq. (13) into Eq. (16), we obtain the relative pressure profiles as

$$\frac{P(z)}{P_{max}} = \left(1 - \frac{z}{z_m}\right)^{n/(n-1)} \tag{17}$$

where P_{max} is the pressure at the bottom of the cake. Thus, for large n such as the case of less strongly flocculated suspensions, e.g., alumina at pH 7.0 where $n/(n-1) = 1.12$ or boehmite at pH 7.0 where $n/(n-1) = 1.33$, $P(z)$ is close to a linear function of z except in the narrow region near the top of the cake. For a small n such as in the case of boehmite at pH 5.5 where $n/(n-1) = 3$, $P(z)$ can no longer be approximated as a linear function of z.

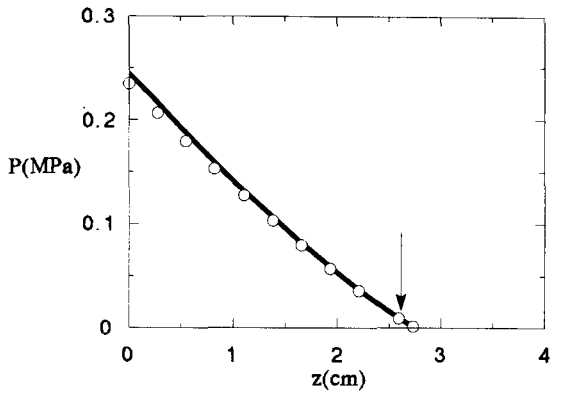

Fig. 7. Pressure profile for the centrifuged cake of alumina at pH 7.0 with $\omega = 241$. The solid line represents $P_s(z)$ and the open circles $P(\phi(z))$, where $P_s(z)$ and $P(\phi(z))$ are as defined in the text.

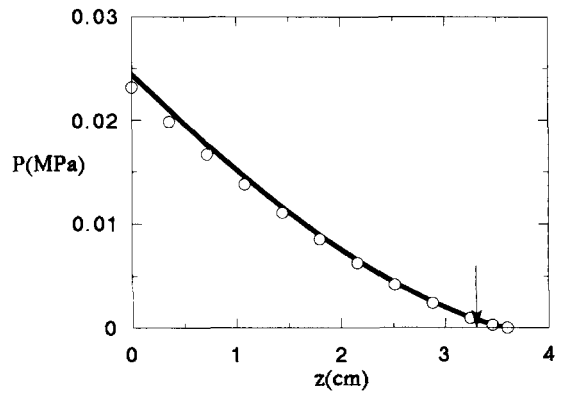

Fig. 8. Pressure profile for the centrifuged cake of boehmite at pH 7.0 with $\omega = 241$. The solid line represents $P_s(z)$ and the open circles $P(\phi(z))$, where $P_s(z)$ and $P(\phi(z))$ are as defined in the text.

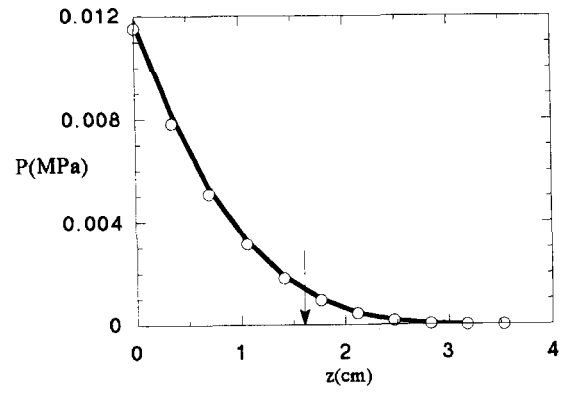

Fig. 9. Pressure profile for the centrifuged cake of alumina at pH 5.5 with $\omega = 241$. The solid line represents $P_s(z)$ and the open circles $P(\phi(z))$, where $P_s(z)$ and $P(\phi(z))$ are as defined in the text.

IV. Concluding Remarks

We have examined the equilibrium-state density profiles of flocculated centrifuged cakes both theoretically and experimentally. Experimentally the density profiles were examined with γ-ray densitometry. Theoretically, the density profiles were obtained by implementing the experimentally obtained power-law pressure–density relationships $P = \beta\phi^n$ into the general differential equations for centrifugation with appropriate boundary conditions. The exponent n in the pressure–density relationship depends on the suspension pH, the characteristics of the particles, and the initial suspension density. The value of n may increase as the cake density increases[8] or as the suspension changes from strongly flocculated, e.g., boehmite suspensions at pH 5.5 where $n = 1.44$ to less strongly flocculated, e.g., boehmite suspensions at pH 7.0 where $n = 4.0$ and alumina suspensions at pH 7.0 where $n = 8.9$.[7,9] We show that the density profiles $\phi(z)$ vs z can be described in a simple form as $\frac{\phi(z)}{\phi_{max}} = \left(1 - \frac{z}{z_m}\right)^{1/(n-1)}$. Thus, the relative density variation within the cake increases as n decreases. The calculated density profiles were shown to be in good agreement with the experimental ones. The relative pressure can be expressed as $\frac{P(z)}{P_{max}} = \left(1 - \frac{z}{z_m}\right)^{n/(n-1)}$

For the same suspension conditions, i.e., with the same n, ϕ_{max} increases and, therefore, z_m decreases with an increasing ω. As a result of the universal dependence of $\phi(z)/\phi_{max}$ on z/z_m, the density gradient actually increases with an increasing ω despite increase in the average cake density.

It should be noted that for the boehmite cakes both at pH 5.5 and at pH 7.0, the P_s–ϕ relationship is best described by the power law depicted in Eq. (3). However, for the alumina cakes, the exponent n in the power-law P_s–ϕ relationship is rather large, i.e., $n = 8.9$. A power-law function with a large exponent is numerically indistinguishable from an exponential one. Indeed, the density ϕ of the alumina cakes can be alternatively fitted as a logarithmic function of P_s or P_s as an exponential function of ϕ.[12] Thus, one may question the validity of using Eq. (13) to describe the density profiles for the alumina cakes, since Eq. (13) is derived using a power-law P_s–ϕ relationship. However, since P_s as an exponential function of ϕ is numerically indistinguishable from that as a power-law one with a large n, the density profiles for the alumina cakes obtained by using an exponential form for P_s would be numerically indistinguishable from those predicted by Eq. (13). The advantage of using Eq. (13) to describe the density profiles of centrifuged cakes is that it provides a simple analytic form for the density profiles through the exponent n that other forms of P_s–ϕ relationship cannot provide.

The form $\frac{\phi(z)}{\phi_{max}} = \left(1 - \frac{z}{z_m}\right)^{1/(n-1)}$ can also be used to describe the density profiles of a sedimentation cake, provided the pressure–density relationship of a sedimentation cake is also a power-law function $P = \beta\phi^n$ (see Appendix A). While the $\left(1 - \frac{z}{z_m}\right)^{1/(n-1)}$ dependence of the relative density $\phi(z)/\phi_{max}$ is an approximation for centrifuged cakes, it is exact for sedimentation cakes.

The uniform density profiles observed in the sedimentation cakes of disperse suspensions[5,6] can also fit this $\frac{\phi(z)}{\phi_{max}} = \left(1 - \frac{z}{z_m}\right)^{1/(n-1)}$ form as explained below. The cake density of dispersed suspensions has been shown to be independent of the applied pressure.[7,9] The independence of the cake density with respect to the pressure means that n is very large if $P = \beta\phi^n$ is used to describe the pressure–density relationship. The large n value gives negligible $\frac{1}{n-1}$ value, therefore, negligible density variations in the main portion of the cake as observed in the density-profile measurements.[5,6]

Finally, in the case of strongly flocculated cakes, especially the ones formed by nanometer-sized particles such as boehmite at pH 5.5, the viscoelasticity of such cakes will allow the cakes to spring back significantly. The springback of the cake may give rise to nonmonotonic density profiles. The density profiles after significant springback are not within the scope of the present paper. The monotonic density profiles predicted by the form $\frac{\phi(z)}{\phi_{max}} = \left(1 - \frac{z}{z_m}\right)^{1/(n-1)}$ are good for cakes that are immediately removed from the centrifugation unit as we have done in the experiment or cakes that do not have significant springback such as alumina at pH 7.0 or boehmite at pH 7.0.

APPENDIX A

The differential equation for sedimentation in the final state is written as

$$\frac{dP_s}{dz} = -\Delta\rho g\phi \tag{A-1}$$

where z is the distance measured from the bottom of the cake. Eq. (A–1) can be rewritten as

$$\frac{dP_s}{\phi} = -\Delta\rho g\, dz \tag{A-2}$$

If the pressure–density relationship of a sedimentation cake is also a power-law function as $P_s = \beta\phi^n$, Eq. (A–2) can be rewritten as

$$\frac{d\phi^n}{\phi} = -\frac{\Delta\rho g}{\beta} dz \tag{A-3}$$

The solution to Eq. (A–3) is

$$\phi(z) = (-c_1 z + c_2)^{1/(n-1)} \tag{A-4}$$

where $c_1 = \frac{n\Delta\rho g}{(n-1)\beta}$ and c_2 is a constant to be determined by the boundary conditions, i.e., Eqs. (7) and (8). By definition, $\phi_{max} = c_2^{1/(n-1)}$ and $z_m = \frac{c_2}{c_1}$. Eq. (A–4) can then be written as

$$\frac{\phi(z)}{\phi_{max}} = \left(1 - \frac{z}{z_m}\right)^{1/(n-1)} \tag{A-5}$$

For sedimentation cakes, the relative density $\frac{\phi(z)}{\phi_{max}}$ also follows the $\left(1 - \frac{z}{z_m}\right)^{1/(n-1)}$ dependence. However, note that this $\left(1 - \frac{z}{z_m}\right)^{1/(n-1)}$ dependence is an approximation for centrifuged cakes but is exact for sedimentation cakes.

APPENDIX B

Nomenclature Table

R	Distance from the center of rotation to the bottom of the cake
r	Position variable measured from the center of rotation
z	Position variable measured from the bottom of the cake
h_0	Initial suspension height
h	Visible cake height
ϕ_0	Initial suspension solid volume fraction
ϕ	Volume fraction of the solid
$\phi(z)$	Local solid volume fraction at position z
ϕ_{max}	Solid volume fraction at the bottom of the cake
ϕ_{ave}	Average solid volume fraction of the cake
P_s	Compressive pressure on the particulate network in the cake
$P_{s,m}$	Mean compressive pressure of the cake
P_{max}	Compressive pressure at the bottom of the cake
n	Exponent for P_s as a power-law function of ϕ
β	Coefficient for P_s as a power-law function of ϕ
ϕ_1	Volume fraction of the fluid
k_0	Ratio of the horizontal compressive pressure to the vertical compressive pressure
$\Delta\rho$	Mass density difference between the solid and the fluid
ω	Angular centrifugation frequency
η	Viscosity of the fluid
κ	Permeability of the cake
q_l	Flux of the fluid
q_s	Flux of the solid
z_m	Distance at which ϕ vanishes
$P(\phi(z))$	Local solid pressure at z calculated as a power-law function of $\phi(z)$
$P(z)$	Local solid pressure at z due to the weight of the cake above z

Acknowledgment: Support by a Drexel Research Scholar Award for W.-H. Shih is acknowledged.

References

[1]R. A. Thompson, "The Mechanics of Powder Pressing: I–III," *Am. Ceram. Soc., Bull.*, **60** [2] 237–45 (1981).

[2]I. A. Aksay and R. Kikuchi, "Structure of Colloidal Solids"; p. 513 in *Science of Ceramic Chemical Processing*. Edited by L. L. Hench and D. R. Ulrich. Wiley, New York, 1986.

[3](a) W. Y. Shih, I. A. Aksay, and R. Kikuchi, "Phase Diagram of Charged Colloidal Particles," *J. Chem. Phys.*, **86** [9] 5127–32 (1987). (b) W. Y. Shih, I. A. Aksay, and R. Kikuchi, "Reversible-Growth Model: Cluster–Cluster Aggregation with Finite Binding Energies," *Phys. Rev. A: Gen. Phys.*, **36** [10] 5015–19 (1987).

[4]F. F. Lange, "Powder Processing Science and Technology for Increased Reliability," *J. Am. Ceram. Soc.*, **72** [1] 3–15 (1989).

[5]C. H. Schilling, G. L. Graff, W. D. Samuels, and I. A. Aksay, "Gamma-ray Densitometry: Nondestructive Analysis of Density Evolution during Ceramic Powder Processing"; pp. 239–51 in MRS Conference Proceedings, *Atomic and Molecular Processing of Electronic and Ceramic Materials: Preparation, Characterization, and Properties*. Edited by I. A. Aksay, G. L. McVay, T. G. Stoebe, and J. F. Wager. Materials Research Society, Pittsburgh, PA, 1988.

[6]F. M. Auzerais, R. Jackson, W. B. Russel, and W. F. Murphy, "The Transient Settling of Stable and Flocculated Dispersions," *J. Fluid Mech.*, **221,** 613–39 (1990).

[7]W.-H. Shih, S. I. Kim, W. Y. Shih, C. H. Schilling, and I. A. Aksay, "Consolidation of Colloidal Suspensions," *Mater. Res. Soc. Symp. Proc.*, **180,** 167–72 (1990).

[8]F. M. Tiller, C. S. Yeh, C. D. Tsai, and W. Chen, "Generalized Approach to Thickening, Filtration, and Centrifugation," *Filtr. Sep.*, **24,** 121 (1987).

[9]W.-H. Shih, J. Liu, W. Y. Shih, S. I. Kim, M. Sarikaya, and I. A. Aksay, "Mechanical Properties of Colloidal Gels," *Mater. Res. Soc. Symp. Proc.*, **155,** 82–92 (1989).

[10]R. Buscall, I. J. McGowen, P. D. A. Mills, R. F. Stewart, D. Sutton, L. R. White, and G. E. Yates, "The Rheology of Strongly-Flocculated Suspensions," *J. Non-Newtonian Fluid Mech.*, **24,** 183 (1987).

[11]W.-H. Shih, W. Y. Shih, S. I. Kim, J. Liu, and I. A. Aksay, "Scaling Behavior of the Elastic Properties of Colloidal Gels," *Phys. Rev. A: Gen. Phys.*, **42,** 4772–79 (1990).

[12]W. Y. Shih, W.-H. Shih, and I. A. Aksay, "Mechanical Properties of Colloidal Gels Subject to Particle Rearrangement," *Mater. Res. Symp. Proc.*, **195,** 477–84 (1990).

[13]S. I. Kim, W.-H. Shih, W. Y. Shih, and I. A. Aksay, unpublished work. □